

# PlutoNet: An Efficient Polyp Segmentation Network

Tugberk Erol, Duygu Sarikaya

**Abstract**—Polyps in the colon can turn into cancerous cells if not removed with early intervention. Deep learning models are used to minimize the number of polyps that goes unnoticed by the experts, and to accurately segment the detected polyps during these interventions. Although these models perform well on these tasks, they require too many parameters, which can pose a problem with real-time applications. To address this problem, we propose a novel segmentation model called PlutoNet which requires only 2,626,337 parameters while outperforming state-of-the-art models on multiple medical image segmentation tasks. We use EfficientNetB0 architecture as a backbone and propose the novel *modified partial decoder*, which is a combination of partial decoder and full scale connections, which further reduces the number of parameters required, as well as captures semantic details. We use asymmetric convolutions to handle varying polyp sizes. Finally, we weight each feature map to improve segmentation by using a squeeze and excitation block. In addition to polyp segmentation in colonoscopy, we tested our model on segmentation of nuclei and surgical instruments to demonstrate its generalizability to different medical image segmentation tasks. Our model outperformed the state-of-the-art models with a Dice score of %92.3 in CVC-ClinicDB dataset and %89.3 in EndoScene dataset, a Dice score of %91.93 on the 2018 Data Science Bowl Challenge dataset, and a Dice score of %94.8 on Kvasir-Instrument dataset. Our experiments and ablation studies show that our model is superior in terms of accuracy, and it is able to generalize well to multiple medical segmentation tasks.

**Index Terms**—Image Segmentation, Deep Learning, Colonoscopy, Histopathology, Surgical Instruments

## I. INTRODUCTION

According to World Health Organisation (WHO), colon cancer is the third most common cancer and the second most deadly cancer. Polyps in colons can turn into cancerous cells and cause colon cancer. For this reason, it is vital that the polyps to be detected and removed with early intervention, before they turn into cancerous cells. Studies show that, during colonoscopy, depending on their type and size, %14-%30 of polyps go unnoticed by the experts [1]. Deep learning models are used to minimize errors, to provide rapid diagnosis and assistance to experts during these interventions. U-Net [2] and similar segmentation models [3]–[5] that use an encoder and decoder structure to capture both the low and high level information, have been widely adopted in medical image segmentation tasks. In PlutoNet, we also adopt an encoder decoder structure, and use EfficientNetB0 architecture [6] as a backbone as it requires fewer parameters while also maintaining a high accuracy on various tasks. Wu et al. [7] show that higher level encoder layers carry both low level and high level features. For this reason, skip connections to the low level features are mostly redundant.

In this work, we propose the novel *modified partial decoder* which is a combination of partial decoder [7] and full scale connections [8]. Using *modified partial decoder*, we are able

to further reduce the number of parameters by ignoring the low level redundant features. Polyps in colonoscopy images have varying sizes, appearances, and aspect ratios. In order to handle these variations, we use asymmetric convolutions in our model. In conventional architectures, all features have the same weights, however, in our model we increase the representation of the more important features. So, we weight each feature map to improve segmentation results by using a squeeze and excitation block. An overview of our model is demonstrated in Figure 1.

We tested our model extensively for the segmentation of polyps in colonoscopy images on five different public datasets. In addition to polyp segmentation in colonoscopy, we tested our model on segmentation of nuclei and surgical instruments to demonstrate its generalizability to different medical image segmentation tasks. To segment polyps in colonoscopy images, we trained our model in Kvasir-SEG [1] and CVC-ClinicDB [9]. We tested our model on ETIS [10], Endoscene [11] and CVC-ColonDB [12]. We tested our model for nuclei segmentation on the 2018 Data Science Bowl Challenge dataset [13], and for surgical instrument segmentation on the Kvasir-instrument dataset [14]. We outperformed the state-of-the-art models with a Dice score of %92.3 in CVC-ClinicDB dataset and %89.3 in EndoScene dataset, a Dice score of %91.93 on the 2018 Data Science Bowl Challenge dataset, and a Dice score of %94.8 on Kvasir-instrument dataset. Our experiments and ablation studies show that our model outperforms state-of-the-art models in terms of accuracy, and it is able to generalize well to multiple medical segmentation tasks. Moreover, our model requires fewer parameters than the state-of-the-art models.

The main points and contributions of our paper can be summarized as below:

- We propose a novel model: PlutoNet.
- We use EfficientNetB0 as a backbone as it requires fewer parameters while also maintaining a high accuracy.
- We propose the novel *modified partial decoder* which is a combination of partial decoder and full scale connections that further reduces the number of parameters required and captures semantic details.
- We use asymmetric convolutions to handle varying sizes, appearances and aspect ratios of polyps.
- We adopt a squeeze and excitation block to increase weights of the more important features to capture precise semantic details.
- To show our model’s generalizability, we tested our model on different medical image segmentation tasks, which are the segmentation of polyps in colonoscopy images, the segmentation of nuclei and the segmentation of surgical instruments.
- Our experiments show that our model outperforms state-

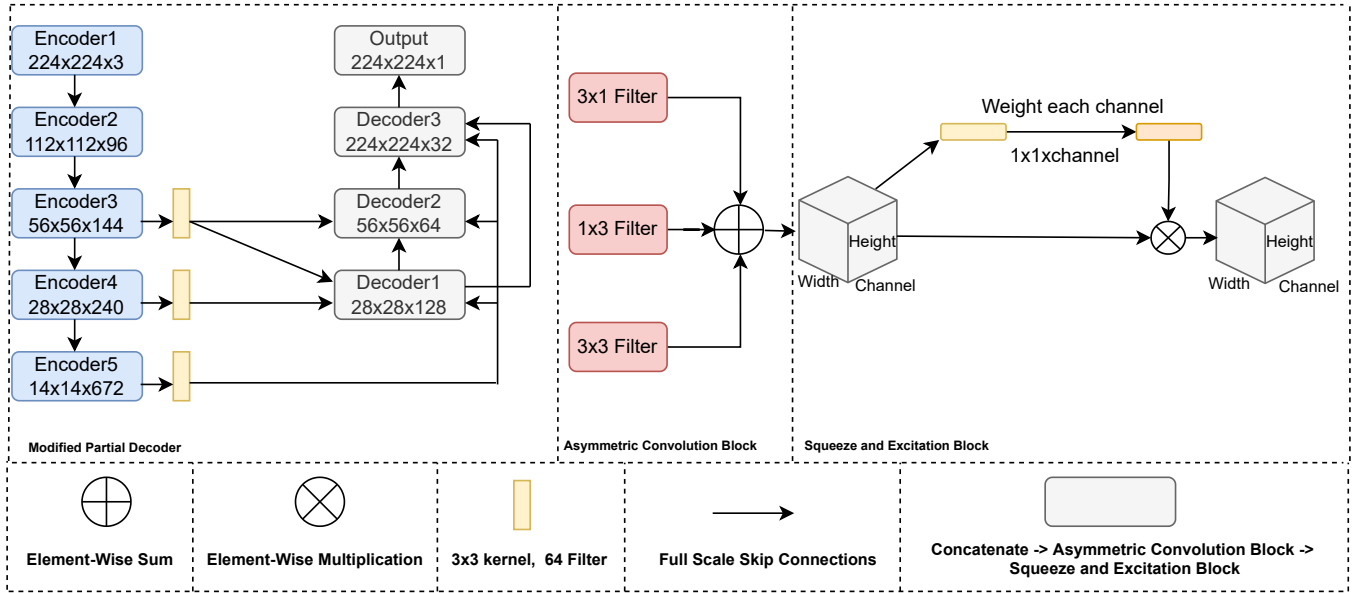


Fig. 1: The overview of PlutoNet. On the left, the encoder decoder structure of our network with *modified partial decoder* is shown. *Modified partial decoder* is a combination of partial decoder and full scale skip connections, and it reduces the number of parameters while capturing semantic details. Decoder layers consist of asymmetric convolutions and a squeeze and excitation block. The middle section shows the details of asymmetric convolutions used in the decoder layers to handle varying appearances, sizes and aspect ratios of polyps. Finally, on the right side, the details of the squeeze and excitation block, which is used to weight each feature map to improve segmentation results, are demonstrated.

of-the-art models in various medical segmentation tasks.

- Our ablation study shows the effectiveness and efficiency of each contribution to our model.

Our paper is organized as follows: In section II, we review the literature for the approaches that are used in medical image segmentation in general, and more specifically for the segmentation of polyps in colonoscopy images and the segmentation of nuclei. In section III, we present our model in detail. In section IV, we give information about the datasets used in experiments, the metrics that are used, and the further details of the experiments. In section V, we share our results and compare our model’s performance with state-of-the-art models. In section VI, we give a brief conclusion of our work and discuss our findings.

## II. RELATED WORK

Ronneberger et al. introduced U-Net [2] which uses an encoder and decoder structure to capture both the low and high level information for medical image segmentation. Due to its success, the encoder decoder structure have been widely adopted and similar models [3]–[5] have been proposed in medical domain.

Jha et al. proposed a model titled ResUNet++ [15] for polyp segmentation in colonoscopy, which is a combination of ResNet [16] and UNet [2]. They used residual blocks to prevent gradient vanishing problem. In addition, ASPP [17] and squeeze and excitation blocks [18] are used. They outperformed U-Net, ResUNet [19] models in CVC-612 and Kvasir-SEG datasets, and achieved highest score in Dice, IoU and recall metrics.

Jha et al. [20] connected two U-Nets, namely, the double U-Net. The main motivation of double U-Net is to capture more semantic details [20]. They carried out experiments on different medical image segmentation tasks including colonoscopy, dermoscopy and nuclei images. They demonstrated that they were able to capture more details by using two connected U-Nets back to back. Zhou et al. [21] proposed a nested U-Net architecture. The main idea behind this work is to redesign skip connection to reduce the gap between encoder and decoder layers. The authors have tested their model on different medical image segmentation tasks that focus on segmentation of nuclei, polyps in colonoscopy, lung nodule and liver, outperforming U-Net on these datasets.

Huang et al. [8] proposed UNET 3+, a U-Net based architecture with full scale connections. The motivation in this study is to capture details and semantics by combining low and high level features at different scales. They used VGG-16 [22] and ResNet-101 [16] as backbone. Wu et al. [7] proposed using cascaded partial decoder for the problem of object detection. Their experiments showed that third encoder layer carried low level features as well as high level ones, therefore concatenations of lower layers are mostly redundant. Based on these findings, they developed partial decoder. In their approach, the features of the first two encoder layers are not used in the attention module. Using partial decoder and attention module, they outperformed state-of-the-art models. Wei et al. [23] proposed a novel polyp segmentation network titled Shallow Attention Network. Following the findings of Wu et al. [7], the authors ignored the connections from the first two encoder layers. To prevent overfitting, they proposed

color exchange. They also developed a probability correction strategy to increase segmentation accuracy in inference time. Meanwhile, Fan et al. [24] introduced a parallel reverse attention network for polyp segmentation. They reduced the number of parameters required by using a parallel partial decoder. They also proposed to use reverse attention [25] to better capture structural details. They demonstrated their model’s results on Kvasir SEG [1], CVC-ClinicDB [9], Etis [10], CVC-ColonDB [12] and Endoscene [11] datasets, and outperformed state-of-the-art models.

Ding et al. [26] developed asymmetric convolutions which strengthen the square convolution kernels. Asymmetric and basic convolutions were tested separately as part of AlexNet [27] and ResNet [16] architectures, and the asymmetric convolutions were shown to be more successful. Hu et al. [18] proposed squeeze and excitation networks. The main idea of this network is to weight each feature map in order to improve representational power of important features. Similarly, Jha et al. [28] proposed a real time polyp segmentation model which consists of residual and squeeze excitation blocks with fewer parameters. Their model demonstrated a significant frame per second (fps) improvement over the state-of-the-art models.

Zhao et al. [29] proposed polyp segmentation model titled MSNET. The Multi-scale Subtraction Module is developed to reduce inaccurate localization and the problem of blurred edges in polyp segmentation, and outperformed state-of-the-art models.

Although the recent advances have been successful in medical image segmentation tasks, the models proposed require too many parameters. This can pose a problem with real time applications such as colonoscopy. In order to address this problem, we propose a novel model titled PlutoNet. We propose the novel *modified partial decoder* which is a combination of partial decoder [7] and full scale connections [8]. Using *modified partial decoder*, we are able to further reduce the number of parameters by ignoring the low level redundant features. In order to handle variations in appearance, aspect ratio and size of the polyps, we use asymmetric convolutions. Finally, we increase the representation of the more important features by weighting each feature map using a squeeze and excitation block. PlutoNet requires only 2,626,337 parameters while outperforming state-of-the-art models on multiple medical image segmentation tasks.

### III. PROPOSED MODEL

we propose a novel segmentation model, PlutoNet, with the motivation to use fewer parameters while maintaining a high accuracy on varying medical image segmentation tasks. We primarily adopt an encoder decoder structure using the last three encoder layers of EfficientNetB0 as the backbone of our network. We propose the novel *modified partial decoder* which is a combination of partial decoder [7] and full scale connections [8]. Using *modified partial decoder*, we are able to further reduce the number of parameters by ignoring the low level redundant features [7]. Inspired by Huang et al.’s work [8], we use full scale skip connections. Full scale skip connections capture feature details at different scales.

We apply 64 convolution filters to the output of the encoder layers, before they go in the full scale connections, which greatly reduces the number of parameters. In order to handle variations in appearance, aspect ratio and size of the polyps, we use asymmetric convolutions. Each decoder layer consists of a asymmetric convolution block followed by a squeeze and excitation block. Our motivation here is to first enrich the feature space using asymmetric convolutions, and then to weight each feature map using a squeeze and excitation block to increase the representation of the more important features.

#### A. Modified Partial Decoder

Full scale skip connections are proposed by Huang et al. [8]. These connections combine low level features and high level features. Integrating low and high level information at different scales minimizes the loss of information. In this work, we also adopted full scale connections, to capture more information at different scales. Wu et al. [7] proposed partial decoder for fast and accurate object detection. The motivation of this work is to show that higher layers contain most of the low level features as well as the high level ones. Most segmentation models with an encoder decoder structure have five encoder layers:  $e^1, e^2, e^3, e^4, e^5$  where the early layers  $e_1, e_2$  extract the low level features and  $e^3, e^4, e^5$  extract the higher level features. Experiments of Wu et al. [7] showed that,  $e^3$  carries low level features, therefore connections to these early layers carry redundant information. Moreover, although  $e^1$  and  $e^2$  require more computations, they contribute less to the overall performance [7]. Based on these findings, in order to reduce the number of parameters of our model, we removed the full scale skip connections of the earlier layers,  $e^1$  and  $e^2$ . This way, we combined partial decoder and full scale skip connections, coming up with *modified partial decoder* which make use of low and high level information at different scales, however reduces the redundant and less informative features coming from the early layers,  $e^1$  and  $e^2$ .

$$\begin{aligned} d1 &= \text{conc}(e^3, e^4, e^5) \\ d2 &= \text{conc}(d^1, e^3, e^5) \\ d3 &= \text{conc}(d^1, d^2, e^5) \end{aligned} \quad (1)$$

In Equation 1,  $\text{conc}$ ,  $d^1$ ,  $d^2$ ,  $d^3$ ,  $e^3$ ,  $e^4$  and  $e^5$  represent concatenate, decoder1, decoder2, decoder3, encoder3, encoder4 and encoder5, respectively. As mentioned earlier, we do not have connections to  $e^1$  and  $e^2$  as the higher layers carry these features making the connections to the two layers redundant.  $e^3$  and  $e^4$  concatenate with the same and larger scale feature maps.  $e^5$  is concatenated with all of the three decoder layers. Also we concatenate inter-decoder layers at larger and smaller scales. These connections are demonstrated in Figure 1.

#### B. Asymmetric Convolution and Squeeze and Excitation Block

Ding et al [26] proposed asymmetric convolutions to strengthen kernels, making them able to handle variations in appearance and size. They experimented with three different state-of-the-art models using asymmetric convolutions, and compared these models to the ones using basic convolutions.

TABLE I: Table shows the datasets we used to evaluate our model on varying medical image segmentation tasks. “# images”, “Image Size” and “Application” represent how many images there are in the corresponding dataset, the width and height information of the images, and the application area that the dataset is collected from, respectively.

Dataset	# images	Image Size	Application
Kvasir SEG	1000	Variable	Colonoscopy
CVC-ClinicDB	612	384x288	Colonoscopy
CVC-ColonDB	380	574x500	Colonoscopy
EndoScene	60	574x500	Colonoscopy
ETIS	196	1225x966	Colonoscopy
2018 Data Science Bowl	670	256x256	Nuclei Imaging
Kvasir-Instrument	590	Variable	Surgery

The models that have asymmetric convolutions outperformed the ones using the basic convolutions. In our work, we use asymmetric convolutions to handle variations in appearance, aspect ratio and size of the polyps. A detailed view of the Asymmetric Convolution block and the Squeeze and Excitation Block can be seen in Figure 1.

$$\text{relu}(\text{bn}(\text{conv}(3 \times 1)) + \text{bn}(\text{conv}(1 \times 3)) + \text{bn}(\text{conv}(3 \times 3))) \quad (2)$$

Equation 2 shows the asymmetric convolution block structure. bn and conv represents batch normalization and convolution, respectively. In decoder layers, we used asymmetric convolutions. Three different convolutions are applied as part of the asymmetric convolution block. After we enrich the feature space using asymmetric convolutions, we weight each feature map using a squeeze and excitation block to increase the representation of the more important features.

#### IV. EXPERIMENTAL DETAILS

We evaluated our model extensively for the segmentation of polyps in colonoscopy images on five different public datasets, and carried out ablation studies to show the effectiveness of each component of our model. In addition to polyp segmentation in colonoscopy, we also evaluated our model on segmentation of nuclei and surgical instruments to demonstrate its generalizability to different medical image segmentation tasks.

The datasets we used to evaluate our model are listed below (Table I):

- Polyp segmentation in colonoscopy images: We use our model to segment the polyps in colonoscopy images. We use Kvasir-SEG, CVC-ClinicDB datasets for training while we use ETIS, CVC-ColonDB and EndoScene datasets for testing.
- Nuclei segmentation: We use our model to segment the nuclei in 2018 Data Science Bowl Challenge Dataset images.
- Surgical instrument segmentation: We use our model to segment surgical instruments in surgical video frames of the Kvasir-Instrument dataset.

#### A. Experiment Details

We followed the experimentation set-up suggested by Fan et al. [24], and splitted Kvasir-SEG and CVC-ClinicDB datasets as % 80 training, %10 validation and %10 testing, and carried out ablation studies on Kvasir dataset. Then we tested our model further on ETIS, CVC-ColonDB and EndoScene datasets to show its generalizability across different datasets. We only use the testing set (CVC-300) of EndoScene.

We tested our model on segmentation of nuclei images using the 2018 Data Science Bowl Challenge dataset. We used %80 of this dataset for training, %10 for validation and %10 for testing. We also tested our model on segmentation of surgical instruments in the Kvasir-Instrument dataset, and used %80 of this dataset for training, %10 for validation and %10 for testing.

We resized all images to  $224 \times 224 \times 3$ . We used common data augmentation techniques which random rotation and horizontal flip in all our experiments.

We trained our model on the Kvasir-SEG, CVC-ClinicDB, and Kvasir-Instrument dataset for 40 epochs. On the other hand, we trained 2018 Data Science Bowl Challenge dataset for 20 epochs. Using validation sets, we set up an early stopping scheme according to the validation loss. We set the initial learning rate to  $1e-4$ . We used Dice loss and Adam optimizer in all experiments.

#### B. Evaluation Metrics

We followed the evaluation metrics suggested by Jha et al. [1], and used Dice coefficient and Intersection over Union (IoU or also as known Jaccard) for our experiments on polyp segmentation. For the rest of our experiments, we used Dice, IoU, AUC, precision and recall metrics.

#### V. RESULTS

For segmentation of polyps in colonoscopy images, we tested our model on the test split of Kvasir SEG [1] and CVC-ClinicDB [9], and on the whole ETIS [10], Endoscene [11] and CVC-ColonDB [12] datasets. We also carried out an ablation study on Kvasir dataset to show the effectiveness of our component of our model.

We tested our model for nuclei segmentation on the 2018 Data Science Bowl Challenge dataset [13], and on surgical instrument segmentation on the Kvasir-instrument dataset [14].

#### A. Polyp Segmentation in Colonoscopy Images

We evaluated our model’s performance with a benchmark consisting of the state-of-the-art models, namely, UNet [2], UNet++ [21], SFA [30], PraNet [24], MSNet [29] and Shallow Attention [23]. TableII shows our model’s performance results for Dice and IoU metrics compared to the results of the benchmark studies. A comparison of the number of parameters each benchmark model requires is also indicated. Figure 2 demonstrates sample segmentation outputs of our model, for all datasets: Kvasir, ClinicDB, Etis, Endoscene, ColonDB, compared to the ground truth.

TABLE II: A comparison of our model’s performance for Dice and IoU metrics to the state-of-the-art models UNet [2], UNet++ [21], SFA [30], PraNet [24], MSNet [29] and Shallow Attention [23] are demonstrated. A comparison of the number of parameters each benchmark model requires is also indicated. According to the results, while our model requires fewer parameters, it achieved the best scores compared to state-of-the-art models with %92.3 Dice score in ClinicDB and %89.3 Dice score in Endoscene datasets (shown in bold).

Methods	Kvasir		ClinicDB		ColonDB		EndoScene		ETIS		Number of Parameters (~) Million
	Dice	IoU	Dice	IoU	Dice	IoU	Dice	IoU	Dice	IoU	
UNet [2]	0.818	0.746	0.823	0.755	0.512	0.444	0.710	0.627	0.398	0.335	15.7
UNet++ [12]	0.821	0.743	0.794	0.729	0.483	0.410	0.707	0.624	0.401	0.344	9
SFA [18]	0.723	0.611	0.700	0.607	0.469	0.347	0.467	0.329	0.297	0.217	-
PraNet [8]	0.898	0.840	0.899	0.849	0.709	0.640	0.871	0.797	0.628	0.567	30.3
MSNET [19]	<b>0.907</b>	<b>0.862</b>	0.921	<b>0.879</b>	<b>0.755</b>	<b>0.678</b>	0.869	0.807	0.719	<b>0.664</b>	27.7
Shallow Attention [20]	0.904	0.847	0.916	0.859	0.753	0.670	0.888	<b>0.815</b>	<b>0.750</b>	0.654	23.9
Ours	0.894	0.808	<b>0.923</b>	0.857	0.718	0.560	<b>0.893</b>	0.806	0.748	0.597	<b>2.6</b>

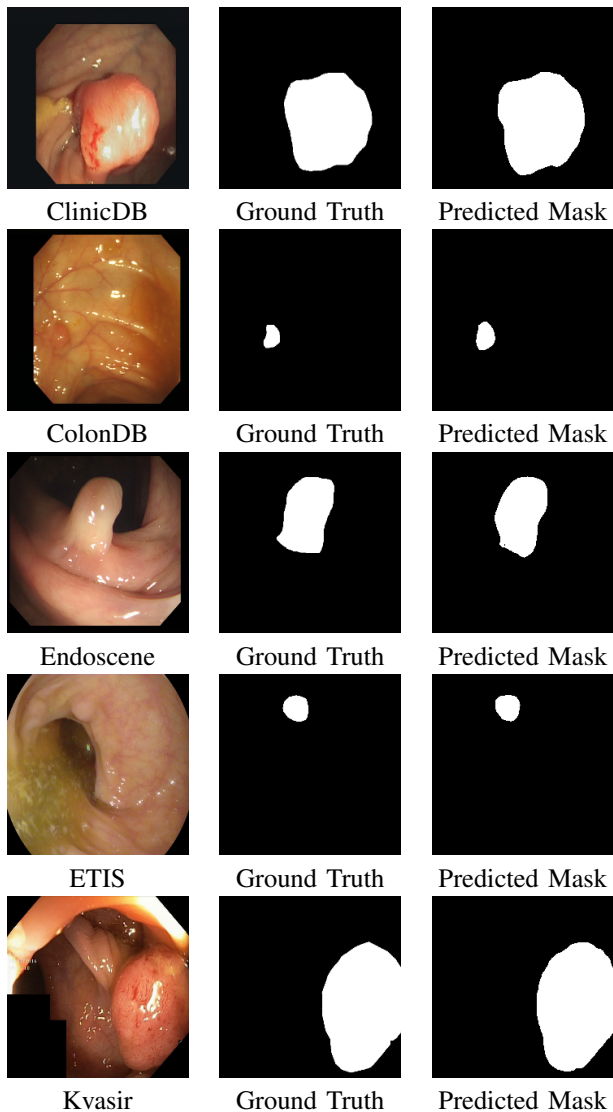


Fig. 2: Sample segmentation outputs of our model, for all datasets: Kvasir, ClinicDB, Etis, Endoscene, ColonDB, compared to the ground truth. As seen in these samples, our model’s segmentation results (predicted masks), are able to capture polyps in different appearances and sizes.

Our model outperformed UNet, UNet++ and SFA on all datasets for Dice and IoU metrics. Even though we used about less than %10 of the parameters required by PraNet, MSNet and Shallow Attention, our model outperformed state-of-the-art models on ClinicDB with a %92.3 Dice score and on Endoscene with a %89.3 Dice score.

### B. Nuclei Segmentation

We evaluated our model’s performance with a benchmark consisting of the state-of-the-art models DoubleU-Net [20], UNet [2] and UNet++ [21]. While DoubleU-Net used VGG19 [22] as backbone, UNet and UNet++ used ResNet101. Table III shows our model’s performance results for Dice and IoU metrics compared to the results of the benchmark studies. Figure III demonstrates sample segmentation outputs of our model, for the 2018 Data Science Bowl Challenge dataset, compared to the ground truth.

Our model outperformed all benchmark studies with a Dice score of %91.93, while the our model requires only 40% of the parameters that are required by the state-of-the-art model that requires the least amount of parameters.

### C. Surgical Instrument Segmentation

We evaluated our model’s performance with a benchmark consisting of the state-of-the-art models U-Net, DoubleU-Net, ResUNet++, NanoNet A [32], NanoNet B [32] and NanoNet C [32]. Table IV shows our model’s performance results for Dice, IoU, AUC, precision and recall metrics compared to the results of the benchmark studies. Figure 4 demonstrates

TABLE III: A comparison of our model’s performance for Dice and IoU metrics to the state-of-the-art models UNet [2], UNet++ [21] and DoubleU-Net [20] are demonstrated. A comparison of the number of parameters each benchmark model requires is also indicated. According to the results, while our model requires fewer parameters, it achieved the best scores compared to state-of-the-art models for the Dice metric (shown in bold).

Method	Backbone	Dice	IoU	# Parameters (~)
U-Net	Resnet101	0.7573	0.9103	7.076.000
U-Net++	Resnet101	0.8974	<b>0.9255</b>	9.004.000
DoubleU-Net	VGG-19	0.9133	0.8407	29.297.570
Ours	EfficientNetB0	<b>0.9193</b>	0.8506	<b>2.626.337</b>

TABLE IV: A comparison of our model’s performance for Dice, IoU, AUC, precision and recall metrics to the state-of-the-art models U-Net, DoubleU-Net, ResUNet++, NanoNet-A, NanoNet-B and NanoNet-C are demonstrated. A comparison of the number of parameters each benchmark model requires is also indicated. Our model outperformed all state-of-the-art models in Dice, IoU and recall metrics (shown in bold), while remaining one of the models that requires fewer parameters.

Method	Backbone	Dice	IoU	AUC	Precision	Recall	Number of Parameters (~)
UNet	-	0.916	0.858	-	0.900	0.949	7.076.000
DoubleU-Net	VGG-19 [22]	0.904	0.843	-	0.897	0.928	29.297.570
ResUNet++	ResNet	0.914	0.864	-	0.935	0.910	4.070.385
NanoNet-A	MobileNetV2 [31]	0.925	0.877	-	<b>0.954</b>	0.914	235.425
NanoNet-B	MobileNetV2 [31]	0.928	0.879	-	0.948	0.920	132.049
NanoNet-C	MobileNetV2 [31]	0.914	0.860	-	0.945	0.903	36.561
<b>Ours</b>	EfficientNetB0 [6]	<b>0.948</b>	<b>0.901</b>	<b>0.969</b>	<b>0.953</b>	<b>0.942</b>	2.626.337

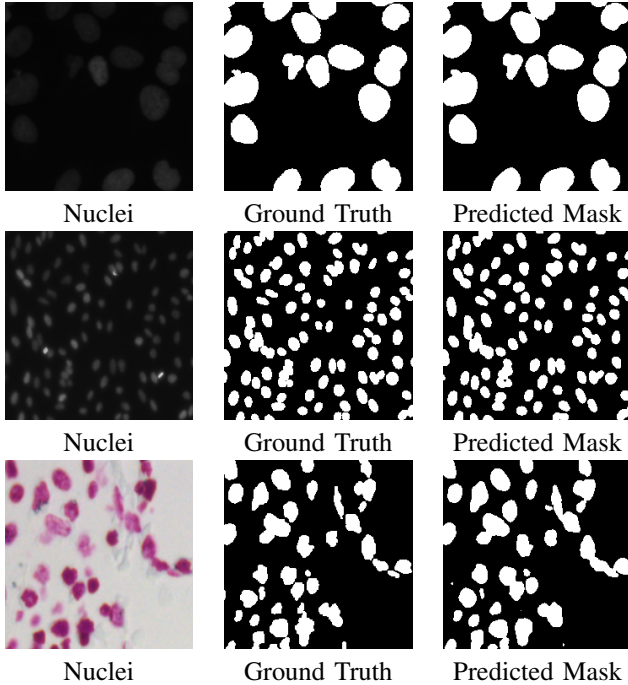


Fig. 3: Sample segmentation outputs (predicted masks) of our model, for the 2018 Data Science Bowl Challenge dataset, compared to the ground truth.

sample segmentation outputs of our model, for the 2018 Data Science Bowl Challenge dataset, compared to the ground truth. Our model outperformed state-of-the-arts models with a Dice metric of %94.8, IoU metric of %90.1 and Recall metric of %94.2, while remaining one of the models that requires fewer parameters.

#### D. Ablation Study Results

We carried out an ablation study on Kvasir dataset to evaluate the effectiveness of each component of our model. First, we used EfficientNetB0 as backbone and used *modified partial decoder*. We achieved a %87.88 Dice and a %78.38 IoU score. Then, in addition to the first part, we added the asymmetric convolution block instead of using the basic convolution block. We reported an improvement of %0.51 Dice and %0.82 IoU score. Figure 5 demonstrates that the added component of asymmetric convolutions were able to capture more semantic information. Afterwards, we integrated squeeze and excitation

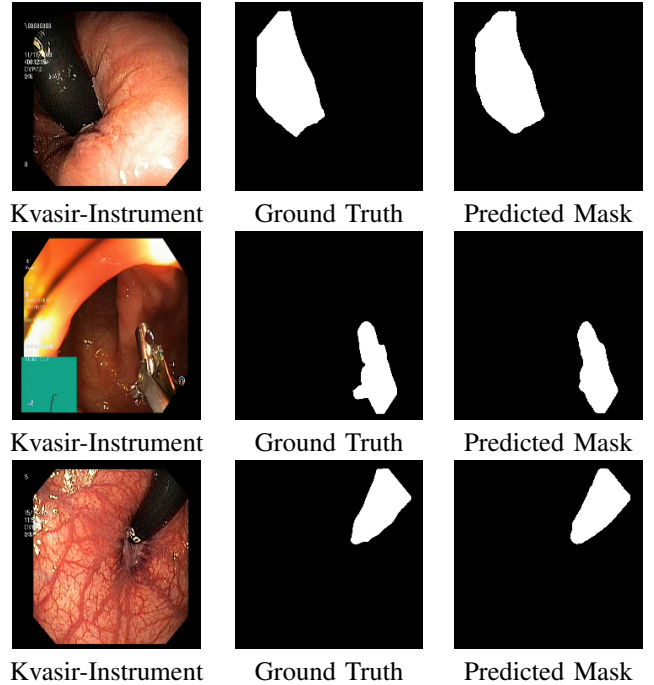


Fig. 4: Sample segmentation outputs (predicted masks) of our model, for the Kvasir-Instrument dataset, compared to the ground truth.

block to the previous model. With combination of asymmetric convolution and squeeze and excitation block, we achieved a %90.97 Dice and a %83.45 IoU score. This led to an improvement of a %2.58 Dice and a %4.25 IoU score. Results of our ablation study can be found in Table V, while sample outputs of each component on the Kvasir dataset can be seen in Figure 5.

## VI. DISCUSSION AND CONCLUSION

Colon cancer is preventable with early intervention where the precancerous polyps are detected and removed before they become cancerous. Deep learning models are used to minimize the number of polyps that goes unnoticed by the experts, and to accurately segment the detected polyps to be removed during these interventions. Recent advances in deep learning are used to assist to the experts during the colonoscopy, however, these models often require too many parameters which may pose a problem with real-time applications, and require high

TABLE V: We carried out an ablation study on Kvasir dataset to evaluate the effectiveness of each component of our model. Backbone represents EfficientNetB0 in our experiment. PD, FSC, ACB and SE represent Partial Decoder, Full Scale Connection, Asymmetric Convolution Block, Squeeze and Excitation, respectively. AS1, AS2 and AS3 stand for Ablation Study 1, Ablation Study 2 and Ablation Study 3, respectively. Using asymmetric convolution block (AS2) instead of using the conventional convolution block (AS1) improved Dice, IoU, AUC and recall scores. Using Squeeze and excitation block with asymmetric convolution block (AS3) achieved the best Dice, IoU, AUC and recall scores which underlines the effectiveness of asymmetric convolutions and squeeze and excitation blocks.

Ablation Study	Dice	IoU	AUC	Precision	Recall	Parameter Sizes
Backbone + PD + FSC (AS1)	0.8788	0.7838	0.8951	<b>0.9534</b>	0.7979	2.192.545
Backbone + PD + FSC + ACB (AS2)	0.8839	0.7920	0.9046	0.9440	0.8188	2.620.961
Backbone + PD + FSC + ACB + SE (AS3)	<b>0.9097</b>	<b>0.8345</b>	<b>0.9306</b>	0.9380	<b>0.8727</b>	2.626.337

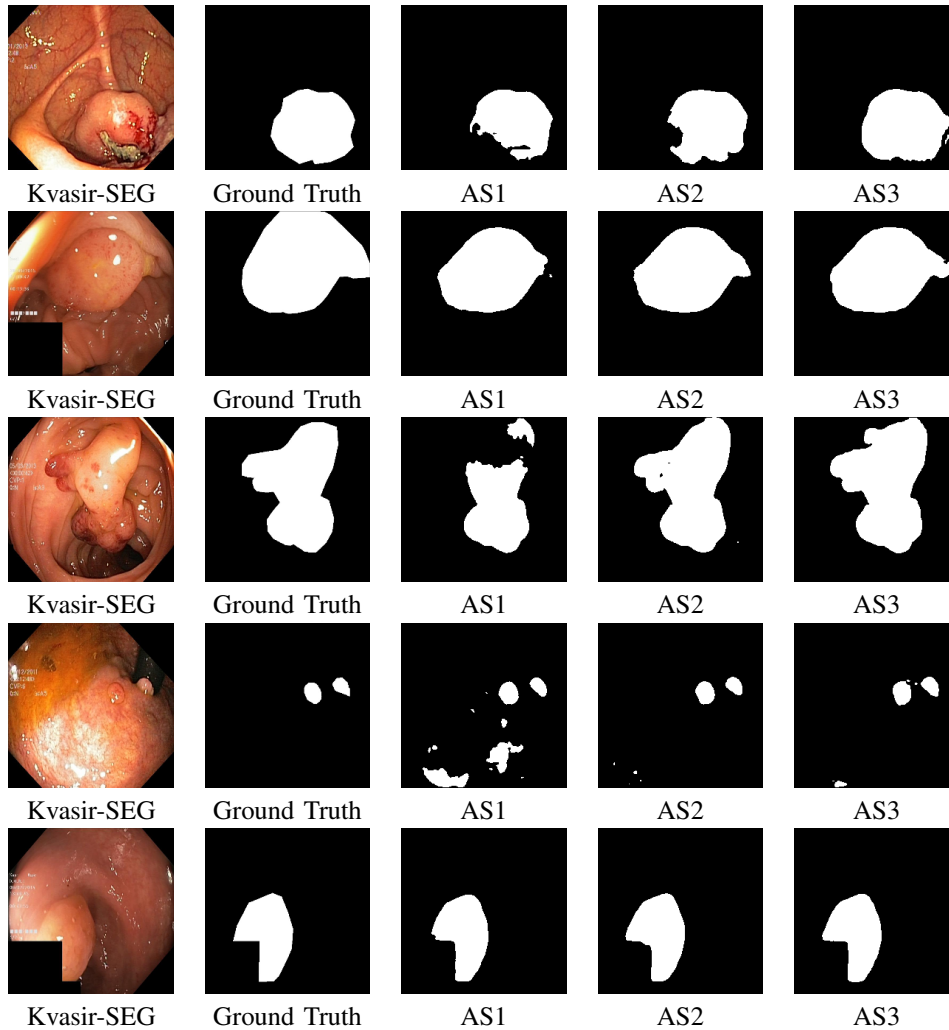


Fig. 5: As part of our ablation studies, sample outputs of each component on the Kvasir dataset are shown. AS1, AS2 and AS3 represent Ablation Study 1, Ablation Study 2 and Ablation Study 3, respectively. AS1 contains Backbone and *modified partial decoder*. Please note how using asymmetric convolution block (AS2) instead of a conventional convolution block (AS1) improved the output by reducing mislocations. An example of this can be clearly observed seen on the fourth row. Adding squeeze and excitation block (AS3) captured more semantic details. Experiment figures show that, using asymmetric and squeeze and excitation block together reduce false negatives and capture more semantic details.

memory usage. We propose a novel model titled PlutoNet, to address these problems. PlutoNet requires only 2,626,337 parameters while outperforming state-of-the-art models on multiple medical image segmentation tasks.

We use EfficientNetB0 architecture as a backbone which achieves a high accuracy while requiring fewer parameters than the state-of-the-art models. We propose the novel *modified partial decoder*, which is a combination of partial decoder and full scale connections. Modified partial decoder further reduces the number of parameters required, as well as captures semantic details at higher and lower levels, without being redundant. We use asymmetric convolutions to handle varying polyp appearances, aspect ratios, and sizes. Finally, we weight each feature map to improve segmentation results by using a squeeze and excitation block. Our ablation study shows using asymmetric convolutions and squeeze and excitation block improve semantic accuracy (Table.V).

Our model requires only 2.626.337 parameters while the state-of-the-art polyp segmentation model which requires the least number of parameters, U-Net++, requires 9.042.177 parameters (TableII). This suggests a substantial improvement over the state-of-the-art.

Our experiments span five different datasets for polyp segmentation in colonoscopy images, as well as two more datasets, 2018 Data Science Bowl Challenge and Kvasir-Instrument datasets, on different medical imaging tasks of nuclei segmentation and surgical instrument segmentation. Our model outperformed UNet, UNet++ and SFA on all datasets for Dice and IoU metrics. Even though we used about less than %10 of the parameters required by PraNet, MSNet and Shallow Attention, our model outperformed state-of-the-art models on ClinicDB with a %92.3 Dice score and on Endoscene with a %89.3 Dice score. Moreover, our model outperformed state-of-the-art models for segmentation of nuclei and surgical instruments, with a Dice score of %91.93 on the 2018 Data Science Bowl Challenge dataset, and a Dice score of %94.8 on Kvasir-Instrument dataset.

## REFERENCES

- [1] D. Jha *et al.*, “Kvasir-seg: A segmented polyp dataset,” in *International Conference on Multimedia Modeling*. Springer, 2020, pp. 451–462.
- [2] O. Ronneberger, P. Fischer, and T. Brox, “U-net: Convolutional networks for biomedical image segmentation,” in *Medical Image Computing and Computer-Assisted Intervention – MICCAI 2015*, N. Navab *et al.*, Eds. Cham: Springer International Publishing, 2015, pp. 234–241.
- [3] V. Badrinarayanan, A. Kendall, and R. Cipolla, “Segnet: A deep convolutional encoder-decoder architecture for image segmentation,” *IEEE Transactions on Pattern Analysis and Machine Intelligence*, vol. 39, no. 12, pp. 2481–2495, 2017.
- [4] O. Oktay *et al.*, “Attention u-net: Learning where to look for the pancreas,” *ArXiv*, vol. abs/1804.03999, 2018.
- [5] X. Li *et al.*, “H-denseunet: Hybrid densely connected unet for liver and tumor segmentation from ct volumes,” *IEEE Transactions on Medical Imaging*, vol. 37, no. 12, pp. 2663–2674, 2018.
- [6] M. Tan and Q. V. Le, “Efficientnet: Rethinking model scaling for convolutional neural networks,” 2020.
- [7] Z. Wu, L. Su, and Q. Huang, “Cascaded partial decoder for fast and accurate salient object detection,” *2019 IEEE/CVF Conference on Computer Vision and Pattern Recognition (CVPR)*, pp. 3902–3911, 2019.
- [8] H. Huang *et al.*, “Unet 3+: A full-scale connected unet for medical image segmentation,” 2020.
- [9] J. Bernal *et al.*, “Wm-dova maps for accurate polyp highlighting in colonoscopy: Validation vs. saliency maps from physicians,” *Computerized medical imaging and graphics : the official journal of the Computerized Medical Imaging Society*, vol. 43, p. 99, July 2015. [Online]. Available: <https://doi.org/10.1016/j.compmedimag.2015.02.007>
- [10] J. Silva *et al.*, “Towards embedded detection of polyps in wce images for early diagnosis of colorectal cancer,” 2016.
- [11] D. Vázquez *et al.*, “A benchmark for endoluminal scene segmentation of colonoscopy images,” *CoRR*, vol. abs/1612.00799, 2016. [Online]. Available: <http://arxiv.org/abs/1612.00799>
- [12] N. Tajbakhsh, S. R. Gurudu, and J. Liang, “Automated polyp detection in colonoscopy videos using shape and context information,” *IEEE Transactions on Medical Imaging*, vol. 35, no. 2, pp. 630–644, 2016.
- [13] C. J.C., G. A., and K. K.W., “Nucleus segmentation across imaging experiments: the 2018 data science bowl,” *Nature Methods*, vol. 16, pp. 1247–1253, 2019.
- [14] D. Jha *et al.*, “Kvasir-instrument: Diagnostic and therapeutic tool segmentation dataset in gastrointestinal endoscopy,” in *MultiMedia Modeling*. Cham: Springer International Publishing, 2021, pp. 218–229.
- [15] —, “Resunet++: An advanced architecture for medical image segmentation,” 12 2019.
- [16] K. He *et al.*, “Deep residual learning for image recognition,” in *2016 IEEE Conference on Computer Vision and Pattern Recognition (CVPR)*, 2016, pp. 770–778.
- [17] L. Chen *et al.*, “Rethinking atrous convolution for semantic image segmentation,” *CoRR*, vol. abs/1706.05587, 2017. [Online]. Available: <http://arxiv.org/abs/1706.05587>
- [18] J. Hu, L. Shen, and G. Sun, “Squeeze-and-excitation networks,” in *2018 IEEE/CVF Conference on Computer Vision and Pattern Recognition*, 2018, pp. 7132–7141.
- [19] Z. Zhang and Q. Liu, “Road extraction by deep residual u-net,” *IEEE Geoscience and Remote Sensing Letters*, vol. PP, 11 2017.
- [20] D. Jha *et al.*, “Doubleu-net: A deep convolutional neural network for medical image segmentation,” 07 2020, pp. 558–564.
- [21] Z. Zhou *et al.*, “Unet++: Redesigning skip connections to exploit multiscale features in image segmentation,” *IEEE Transactions on Medical Imaging*, vol. 39, no. 6, pp. 1856–1867, 2020.
- [22] K. Simonyan and A. Zisserman, “Very deep convolutional networks for large-scale image recognition,” 2015.
- [23] J. Wei *et al.*, “Shallow attention network for polyp segmentation,” in *MICCAI*, 2021.
- [24] D.-P. Fan *et al.*, “Pranet: Parallel reverse attention network for polyp segmentation,” in *Medical Image Computing and Computer Assisted Intervention – MICCAI 2020*, A. L. Martel *et al.*, Eds. Cham: Springer International Publishing, 2020, pp. 263–273.
- [25] S. Chen *et al.*, “Reverse attention for salient object detection,” *CoRR*, vol. abs/1807.09940, 2018. [Online]. Available: <http://arxiv.org/abs/1807.09940>
- [26] X. Ding *et al.*, “Acnet: Strengthening the kernel skeletons for powerful cnn via asymmetric convolution blocks,” in *The IEEE International Conference on Computer Vision (ICCV)*, October 2019.
- [27] A. Krizhevsky, I. Sutskever, and G. E. Hinton, “Imagenet classification with deep convolutional neural networks,” in *Advances in Neural Information Processing Systems*, F. Pereira *et al.*, Eds., vol. 25. Curran Associates, Inc., 2012.
- [28] D. Jha *et al.*, “Real-time polyp detection, localization and segmentation in colonoscopy using deep learning,” *Ieee Access*, vol. 9, pp. 40496–40510, 2021.
- [29] X. Zhao, L. Zhang, and H. Lu, “Automatic polyp segmentation via multi-scale subtraction network,” in *MICCAI*. Springer, 2021.
- [30] Y. Fang *et al.*, “Selective feature aggregation network with area-boundary constraints for polyp segmentation,” in *Medical Image Computing and Computer Assisted Intervention – MICCAI 2019*, D. Shen *et al.*, Eds. Cham: Springer International Publishing, 2019, pp. 302–310.
- [31] M. Sandler *et al.*, “Mobilenetv2: Inverted residuals and linear bottlenecks,” in *2018 IEEE/CVF Conference on Computer Vision and Pattern Recognition*, 2018, pp. 4510–4520.
- [32] *NanoNet: Real-Time Polyp Segmentation in Endoscopy*. IEEE.